

# ATIC: Automated Testbed for Interference Testing in Communication Systems

Michelle Pirrone<sup>†,\*</sup>, M. Keith Forsyth<sup>†</sup>, Jordan Bernhardt<sup>†</sup>,

Daniel Kuester<sup>†</sup>, Aric Sanders<sup>†</sup>, Duncan McGillivray<sup>†</sup>, Adam Wunderlich<sup>†</sup>

<sup>†</sup>Communications Technology Laboratory, National Institute of Standards and Technology, Boulder, Colorado USA

<sup>\*</sup>Department of Electrical, Computer, and Energy Engineering, University of Colorado Boulder, Boulder, Colorado USA  
 {michelle.pirrone, keith.forsyth, jordan.bernhardt, dan.kuester, aric.sanders, duncan.a.mcgillivray, adam.wunderlich}@nist.gov

**Abstract**—The proliferation of communication devices and systems has led to increasingly complex and dynamic spectral environments. This greatly impacts the operations of a multitude of organizations, including commercial entities, academic and non-commercial scientific research, and military equipment and missions, where devices such as cellular systems, radar, and Wi-Fi may share the same spectrum space. The automated testbed for interference testing in communication systems (ATIC) provides a low-cost, flexible framework to perform repeatable, well-controlled interference susceptibility testing with a wide variety of “closed-box” communication systems. Examples of closed-box systems that could be evaluated with ATIC include aeronautical mobile telemetry, microwave point-to-point, and WiFi-like systems. Using relatively inexpensive commercial-off-the-shelf (COTS) components, this testbed provides insight into the resilience of communication systems against external interferers, both friendly and hostile, helping inform decisions on spectrum management and deployment of new technologies. This paper provides a systematic approach to executing interference testing via a simple, streamlined setup with example electronics provided. Additionally, guidelines for testbed validation are demonstrated and open source code is provided for rapid, repeatable implementation.

## I. INTRODUCTION

The pervasive and diverse use of communication devices increases the risk of radio frequency (RF) interference between systems. This issue is further exacerbated by different versions or products within the same technology regime that have widely varying behaviors or responses to interference, which is a concern for consumer products, scientific research, and military operations. Military systems have also needed to address the reallocation and repacking of frequency band allocations, particularly over the last ten years, that has seen consumer devices sharing the same frequency bands or operating in adjacent bands [1], [2].

Interference, whether from friendly or hostile devices, can hamper communication throughput or totally compromise a link, which is especially dangerous to mission critical operations [3]. The increase of communication devices, the sharing of frequency bands, and the rapid deployment of new devices and protocols have been challenging issues and have driven demand for cost-effective, practical, and quickly implemented methods to perform susceptibility and resiliency testing to interference on preexisting and new technologies [4], [5].

*U.S. government work, not protected by U.S. copyright.*

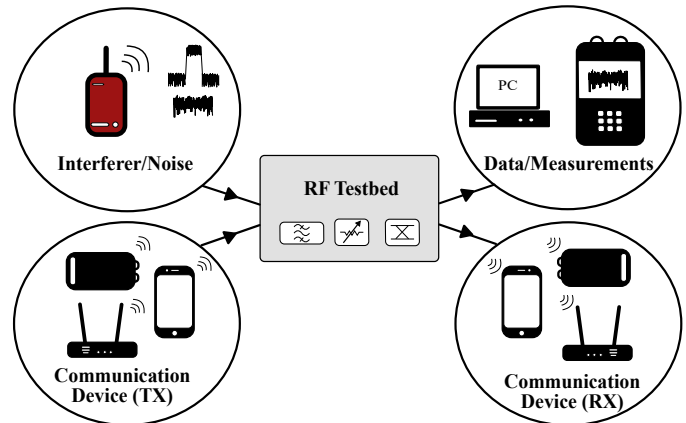


Figure 1. Conceptual, generalized overview of the testbed.

The automated testbed for interference testing in communication systems (ATIC) and the framework for testing presented in this paper provide a low-cost, accessible methodology to setup, validate, and run experiments for general-purpose, noise and interference susceptibility assessment, integrating automation for efficient operation and repeatability. Performance validation on both a component and system level is a crucial step in setting up and operating a testbed to substantiate experimental results. The testbed and operating principles are demonstrated using readily available commercial-off-the-shelf (COTS) components. This includes integrating a software-defined radio (SDR) to enhance the cost-effectiveness of the system; a topic previously studied in [6]. The testbed software and validation data from this work are publicly available<sup>1, 2</sup>.

The emphasis of our test approach is on a simple and efficient, automated testing applicable to a wide variety of closed-box communication devices. The testbed design and accompanying software enable users to quickly stand-up their own setup and run experiments. Measurements can be performed systematically with little operator input and auxiliary scripts can perform data analysis directly on the results. A conceptual overview of this system is shown in Fig. 1. Although an example testbed with particular components is shown here,

<sup>1</sup><https://github.com/usnistgov/atic>

<sup>2</sup><https://doi.org/10.18434/mds2-3070>

our primary aim is to develop a structured, general-purpose framework for setting up interference susceptibility tests, in which users can easily substitute specific equipment or change experimental factors with little additional overhead.

The design and operation of ATIC is motivated by traditional rate vs. range tests as well as blocking (desensitization) testing commonly used for communication devices. In rate vs. range testing, the TX and RX components of a bidirectional communication link are isolated and connected via conducted circuit through a variable attenuator and the variation of a metric such as throughput is measured as the attenuation is changed [7], [8]. Often, propagation channel effects are incorporated in testing, which has drawbacks of increasing test complexity and associated uncertainties. Instead, ATIC uses variable attenuators as a controlled surrogate for physical range to simplify and quickly implement testing, decreasing testing variation and enhancing repeatability. Desensitization of receivers can be measured by sending a signal of constant power through the link and introducing a known interference signal with a tunable power level to the system to observe the degradation in link quality and performance [9]. ATIC facilitates these commonly used tests via a configurable setup by providing multiple tunable elements, the ability to inject both noise and structured interference, and multiple circuit test points. Prior laboratory-based interference investigations by some of the authors were additionally leveraged in the development of this testbed [10]–[12]; a similar application of range testing was presented in [13].

## II. TESTBED OVERVIEW

The ATIC framework was designed to be compatible with a variety of communication devices, provide a wide range of test conditions, and allow measurements and validation checks throughout the circuit. Additionally, the desire for an accessible testbed setup determined the selection of inexpensive COTS components in the circuit. A diagram of the physical layout of the RF circuit is shown in Fig. 2. The TX and RX branches of the hardware are contained in two, separate enclosures to ensure isolation between these two branches and from external signals that may be present. This isolation is critical to mitigate any impacts of additional communication devices in the nearby vicinity and ensure the link is communicating through the conductive setup.

The RF hardware was additionally chosen to maintain reciprocity in the setup. Therefore, the TX and RX devices could be switched to operate as the other side of the link with the hardware enabling the same behaviors and response to occur. Due to this reciprocity, measurements can be taken on both sides of a bidirectional link to provide additional insights including validating impacts from interferers and RF isolation. Performance testing, such as with closed-loop testing, would be possible with this testbed.

Assessments of system behavior can be measured from the directional coupler, the dual directional coupler, and the output of the system (RX port). Measurements taken at the directional coupler can verify the output of the noise or interferer source

along with the combination of these if they are operated at the same time. The dual directional coupler test port allows characterization of the combination of the TX signal with the noise/interference independent of using the RX device for key performance indicators (KPIs) and measurements. These two ports are mainly for diagnostics and additional collection of data for validation purposes. The data pulled from the RX communication device acts as the main hub for test results.

The testbed was initially configured for tests in the 6 GHz WiFi 6e frequency band, but it can easily be modified to operate in other frequency bands. ATIC as demonstrated here is in a conducted, wired configuration, but could be modified for over-the-air, wireless testing with the addition of antennas at the threshold between the enclosures and an expanded set of validation measurements. Key features of an example ATIC implementation are described below.

### A. Software Defined Radio Integration

An Ettus X410<sup>3</sup> software defined radio (SDR) was integrated into the testbed to generate noise and interference waveforms [14]. This device is relatively low cost, while maintaining an appropriate frequency range and having a variety of useful features. These include a frequency range from 1 MHz-8 GHz, a maximum bandwidth of 400 MHz, a maximum output power of 23 dBm (dependent on frequency), simultaneous TX/RX signals, internal temperature sensors (for system stability validation), and custom interfacing in the internal front-end circuit. These features are useful both for running a variety of tests and also for validating the quality of the tests. This device can easily be substituted with another SDR while maintaining overall functionality of the test circuit (with the exception of some more specific features such as internal temperature sensing, which will be dependent on device). The X410 can be treated as a socket server and a driver was developed to interface with this socket and control the device using Python scripts.

### B. Point to Point Link

A LigoWave LigoPTP 6-N RapidFire point-to-point (P2P) link was used as an example “closed-box” communication system [15]. This device operates in the U-NII-5 6 GHz band (5.925-6.425 GHz) and can be configured to employ one of several channel bandwidths (5, 10, 20, 40, 80 MHz) in single spatial stream operation. The additional option of dual spatial streaming is available. The device has binary programs that can be directly accessed through a secure shell to assess a multitude of KPIs of the system. In this work, data throughput was the primary KPI. A maximum TX power level of 30 dBm can be obtained with this link. Binaries from the communication link allow data to be pushed unidirectionally, from parent to child device, as was done in this testbed.

<sup>3</sup>Certain commercial products or company names are identified here to describe our study adequately. Such identification is not intended to imply recommendation or endorsement by the National Institute of Standards and Technology, nor is it intended to imply that the products or names identified are necessarily the best available for the purpose.

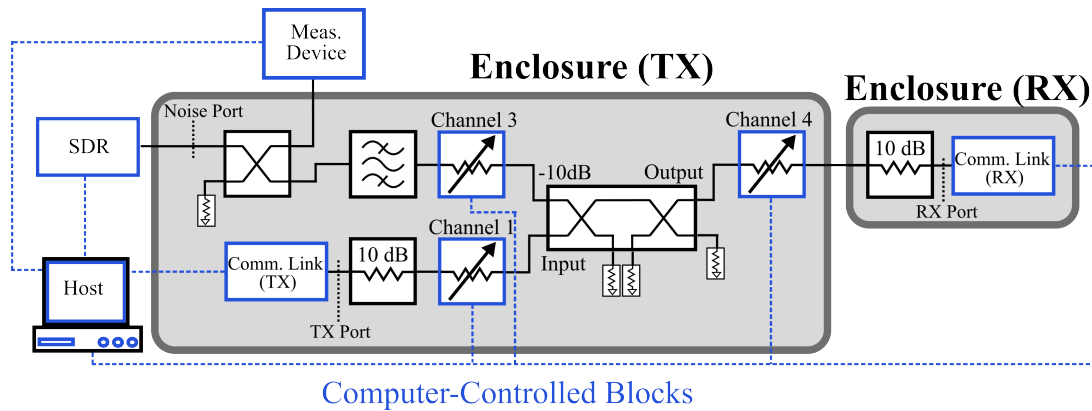


Figure 2. RF hardware setup of testbed, including components that interface with software.

### C. Variable Attenuator

A variable attenuator is included in the testbed to enable simple automated control of path losses that would occur in a wireless environment. Specifically, a MiniCircuits, 4 port, 95 dB programmable attenuator (RCDAT-8G-95) [16] was used for this setup as shown in Fig. 2. The variable attenuations on different branches of the circuit simulate path loss caused by physical distance in either the communication link or from the noise/interference source. A channel emulator could be used in place of the variable attenuator. However, it can be challenging to pick appropriate fading channel models for specific communication systems or representative environmental conditions. Moreover, channel emulators add additional experimental variability, making it more difficult to perform well-characterized, repeatable tests. Therefore, a variable attenuator was used in this testbed to simplify experimentation and facilitate repeatability.

The testbed configuration depicted in Fig. 2 uses three of the four channels in the variable attenuator, with a single channel used for both the noise and interference branch. This could easily be modified to allocate one channel for each branch, allowing for more nuanced control in noise and interference testing. The insertion loss of the device at the U-NII-5 6 GHz band is approximately 8 dB, with up to an additional 95 dB possible to add to the branches of the system. The variable attenuator has an accuracy of 0.25 dB and a tune time of less than 1 ms, allowing for relatively quick changes. Isolation between channels is a minimum of 100 dB and typically on the order of 125 dB.

### III. SOFTWARE CONTROL

The development of software for automated control of the testbed focused on a streamlined, easily modifiable process that used open-source programs and languages. This included automation control over each of the instruments and communication links when possible and the design of the overall workflow of experimentation.

An overview of the networking used in the testbed setup is shown in Fig. 3. A central host (PC) was assigned as the main control hub for all of the software implementation.

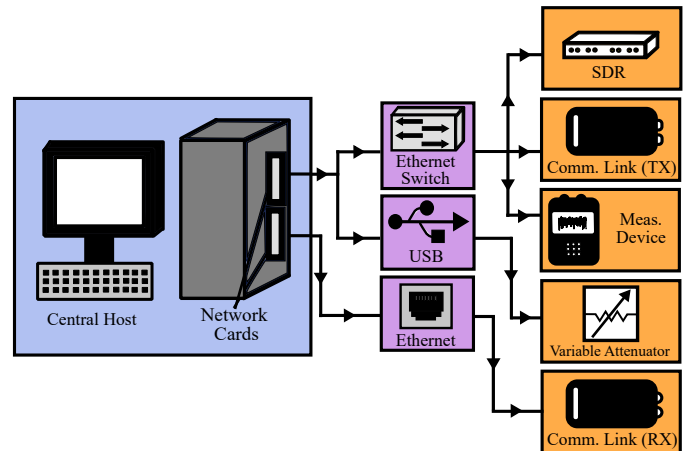


Figure 3. Networking used for testbed setup.

This hub was used to communicate with devices in the RF circuit along with both the TX and RX channels. As the TX and RX branches of the communication link needed to be isolated in software for independent testing and to prevent unintended cross-talk, two separate network cards within the host were utilized. On the TX side of the network, Ethernet protocol was used to communicate with the SDR, the TX communication link, and any additional measurement devices, such as a power sensor. This was done through an Ethernet switch. Additionally on the TX side, the host connected to the 4 port attenuator with USB, which powered the device and allowed communication. On the RX branch, a separate Ethernet network card interfaced with the RX communication link on an isolated subnet.

A flow diagram for experimental execution is shown in Fig. 4. The overall process ingests input variables, runs a set of tests (referred to in total as an experiment), and records the output KPIs of the tests. Specifically, ATIC tests are established through two files: `testbed-conditions` and `configuration`. The configuration file specifies high-level parameters such as networking addresses, result file locations and the X410 test environment. The

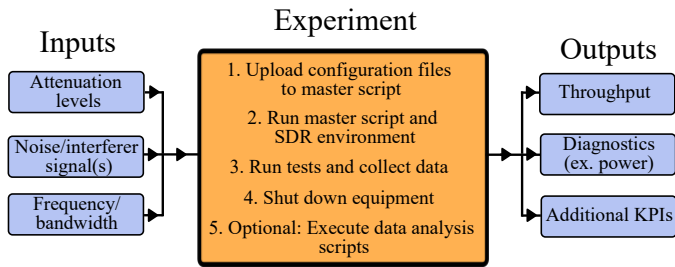


Figure 4. Flow diagram of experimentation.

testbed-conditions file includes test factor settings, e.g., attenuation, power levels, bandwidth, frequency. An additional metadata file can be included to summarize the purpose of the experiment and is recommended to maintain organization amongst multiple experiments.

Once the test configuration files are prepared, they are accessed by a master testbed script within the central host for experimentation to proceed. As an experiment runs through each test configuration (as determined in the testbed-conditions file), the results are stored in an allocated folder. This collection includes KPI reports from the RX device, e.g., throughput, along with additional measurements taken for validation or monitoring of the system, such as power measured at the directional coupler diagnostic port near the noise/interference input or internal temperature monitoring of the SDR. When the experiment is completed, the master script automatically shuts off all devices. Additional analysis steps may be included in this process through scripted generation of data visualization or summary data sets based on test file results.

#### IV. SDR CHARACTERIZATION

Several tests were performed to characterize the behavior of the X410 SDR and monitor its output stability and quality. These tests were used to confirm the effective implementation of the X410 in the testbed for interference measurements and should be performed in general on any device used to generate interference or noise in susceptibility testing. Initial measurements of the output power on the X410 were first performed to confirm the range of linear, stable operation of the device. Output power levels were varied from -5 dBm to 25 dBm in steps of 5 dB and the power spectrum at intervals of 1.25 MHz were recorded using a spectrum analyzer. The bandwidth of the test was from 2 to 13 GHz, to check for harmonics and lower frequency instabilities that occur. Even though behaviors seen at much higher or lower frequencies than the operation frequency could be filtered out, they can be indicative of degradation in overall system performance, including in the frequency band of interest. This was performed both for an additive white Gaussian noise (AWGN) noise signal with a channel bandwidth of 30 MHz centered at 6.02 GHz and a single tone centered at 6.02 GHz.

For the AWGN noise validation tests, the median amplitude of the generated signal in the bandwidth of operation was

recorded for each output power level. The generated output of the X410 began to saturate for gain settings above 15 dB, consistent with the manufacturer's specifications. Additionally, the power spectrum of the single tone test was analyzed for each output power level, showing that potential intermodulation products began to appear at the 10 dB output gain setting. Therefore, we limited the X410 output gain setting to a maximum of 10 dB.

The output power and the temperature of the X410 were additionally characterized to assess stability over time and during startup operations. Namely, the X410 signal generation was operated continuously for 12 hours at a constant output power setting (5 dBm), generating an AWGN signal with a bandwidth of 30 MHz. For the duration of this test, the temperature of the motherboard and daughterboard inside of the X410 along with the output power in the band of operation were recorded every 100 seconds using the internal temperature sensors of the X410 and an external power sensor. This test showed that the internal temperature only varied by a maximum of 1°C over 12 hours. Additionally, the output power had a maximum variation of 0.64 dB, i.e.,  $\pm 0.32$  dB around the median value, which is within the expected level of uncertainty for the measurement devices used.

Another 12 hour test analyzed the fidelity of the X410 output power at startup. The transmit signal of the X410 was turned on (AWGN at a bandwidth of 30 MHz), run for 100 seconds, and turned off. Then, the on-off cycle was repeated for 12 hours. It was found that the bandwidth output power level for this experiment at the end of each test varied by at most 0.73 dB. Therefore, the X410 was validated as a noise or interference source for a power accuracy of within 1 dB for both startup power level fidelity and consistent power levels.

#### V. RF CIRCUIT MEASUREMENTS

Measurements of the RF circuitry were performed to calibrate link power quantities, establish physical repeatability, and validate hardware operation. Typically, an estimate can be made of the insertion losses and isolation that will occur through a system based on the datasheets of the components used in the setup. However, performing measurements with a vector network analyzer (VNA) enables quality assurance of the testbed and initial troubleshooting, if required.

The test circuit was measured with a VNA (Rohde and Schwarz ZNB8) to record reflection losses, insertion losses, and isolation between the noise and TX port. In particular, measurements were taken when the variable attenuator channels were set to 0 dB, or maximum operating power conditions for testing the link. Typically, small reflection coefficients (on the order of less than -10 dB) are desired to minimize mismatch losses between components. Reflections were found to be acceptable at each of the ports; at 6.02 GHz (center frequency of operation), they were the following: -14.9 dB at the TX port, -17.5 dB at the noise port, and -24 dB at the RX port. Further, within the frequency range of the filter (4.9-6.2 GHz), the highest reflection value for each of the ports was -13.5 dB at the TX port, -10.3 dB at the noise port, and -22 dB

at the RX port, verifying the testbed acceptably performed for the entirety of its operable frequency range. Isolation between the noise and TX port was 67.8 dB at 6.02 GHz and the insertion loss from the TX to RX port was 44.6 dB.

The insertion gain between the noise port and RX port was more thoroughly investigated to illustrate the importance of performing a VNA measurement in a testbed setup. A comparison was made for three different scenarios: an estimate of the insertion gain for the testbed based on the datasheets of the components used, an actual measurement, and a representative example of a faulty component in the system using a reverse polarity SMA (RP-SMA) connector incorrectly mated with an SMA connector. The results are shown in Fig. 5.

The difference between the estimated results and the measured results under normal testbed conditions was 7.5 dB, mainly attributed to losses in the relatively low-cost connectors and cables used. Therefore, in a physical system, performing a quick VNA measurement is necessary for accurate results. Components like connectors and cables add additional losses (roughly on the order of 0.5-1.0 dB) that are difficult to model and device performance may vary from their datasheets dependent on test conditions and manufacturing variation. This variation between estimated and actual results would also be difficult to de-embed from communication link behavior during operation.

Furthermore, accidentally placing a wrong connector, such as the reverse polarity connector in this example, decreased the insertion gain by 13 dB, a significant difference in performance. This would be similar to including an SMA connector with a broken center pin. A malfunctioning, inappropriate, or broken RF component, even a passive one, can accidentally be included in the setup and either break the system or deteriorate performance significantly, as was shown. It may also lead to inconsistent losses and varying performance issues over time. Therefore, testbeds such as the one demonstrated here greatly benefit from quick and easy checks with a VNA to ensure a quality test circuit that is operating as intended.

## VI. VALIDATION OF THE TESTBED

For any testbed that follows the basic structure here, once the interference/noise source and the RF hardware is characterized, the entire testbed, including automation software, should be validated. To this end, additional tests were performed to assess consistency of the communication link under different conditions and to verify testbed control.

The first validation test was performed with the communication link under a condition of no added noise or interference, using a bandwidth of 20 MHz and a single antenna port. The consistency of the combined setup, using the steady-state throughput of the communication link as the metric, was measured for six attenuation settings applied to the TX signal: 0, 25, 30, 35, 40, and 45 dB, which were selected based on previous knowledge of where the communication link had reduced throughput. Each test condition was repeated 96 times, where the steady-state throughput was measured for 300 seconds and averaged. The throughput varied by less than

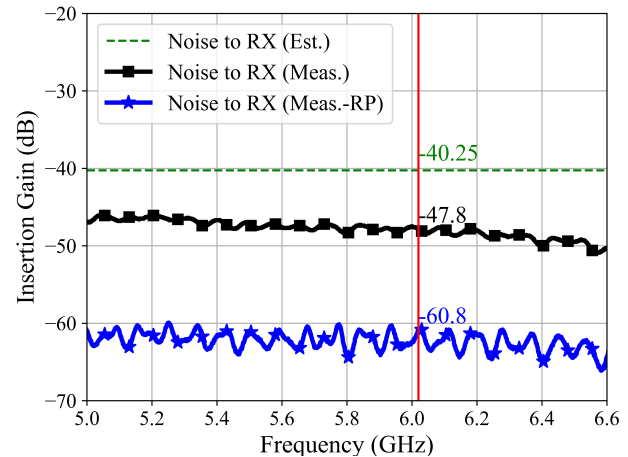


Figure 5. Estimated (green/dashed line) and actual (black/square) measurements of insertion gain from the noise port to the RX port, as well as insertion gain when an “accidental” reverse polarity (RP) connector is placed in the circuit (blue/star). Red line indicates center operation frequency (6.02 GHz).

1 Mbps for all but the 25 dB attenuation case. For the 25 dB attenuation condition, the throughput varied by a maximum of 5.8 Mbps. The greater variation in this case may have been caused by proximity to a transition region between the modulation and coding index values, which were automatically set by the P2P link. The maximum standard deviation seen for these tests was 2.02 Mbps for the 25 dB attenuator setting and 0.14 Mbps across all other cases. Overall, the results indicated that the communication link was very stable and consistent in performance and that the control software was reliable over a total of  $6 \times 96 = 576$  test configurations.

The second validation test assessed throughput with a constant TX power level over various levels of added noise or interference, using channel 3 of the attenuator as shown in Fig. 2 to control the added noise/interference level. This is equivalent to increasing or decreasing the noise power or emulating a variable distance of an interferer. In this test, the SDR generated either AWGN or a previously recorded LTE waveform, and the interferer attenuator was varied from 90 dB to 0 dB in steps of 2 dB. The AWGN noise waveform generated at the output of the SDR had a channel power of -10.9 dBm, as verified by a signal analyzer. The LTE signal was taken from a published dataset of field captures of multi-UE AWS-1 LTE [17], [18], where the particular capture selected contained a relatively high amount of LTE traffic. A 500 ms segment of the LTE signal was extracted from the original five second capture and downsampled from the original 46.08 MHz bandwidth to 30.72 MHz, in order to stay within the memory and sample rate constraints of the SDR. The LTE capture segment had a channel power level over 500 ms of -29.4 dBm, and a peak to average power ratio (PAPR) of 17.06 dB.

For this test, the TX attenuation was set to a constant 23 dB, which was selected to allow for throughput degradation over the course of the test, where the maximum throughput of the

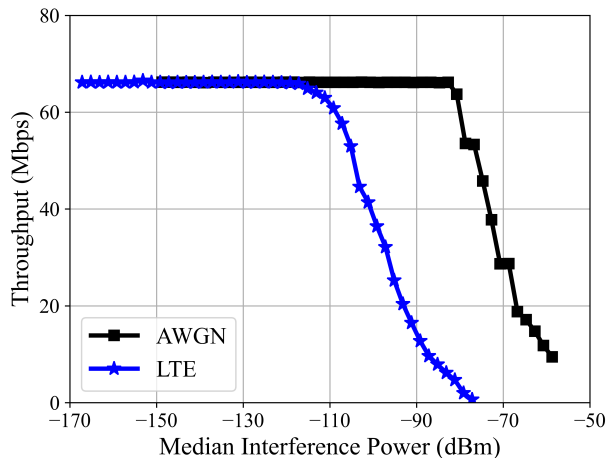


Figure 6. A comparison of the averaged throughput when applying AWGN (black/square) or an LTE signal (blue/star) with varying attenuation levels. The power was referenced to the RX port, as labeled in Fig. 2.

link was approximately 66 Mbps. The RX attenuation was set to 0 dB and the packet size was set to 1600 bytes. A wait time of 10 s was implemented for each test configuration before starting data collection on the testbed, to allow the link to reach a steady-state condition. The testbed control software has the option to randomize the test order of experimental conditions, a recommended practice for experimentation that alleviates potential systematic bias from uncontrolled, extraneous factors [19]. Test conditions were randomized for the entire validation experiment. A Python script processed throughput data, made plots, and saved a summary file of test statistics.

Fig. 6 shows the resultant behavior from the second validation test. Due to the preliminary nature of the validation tests, insufficient replications were collected to rigorously assess uncertainties. However, these preliminary results indicated test stability, and a full uncertainty evaluation will be carried out in future experiments. A stepped throughput response was observed in the AWGN results, while a similar, but smoother response curve resulted from using an LTE signal as the interferer. The stepped response in the presence of the stationary AWGN is indicative of modulation and coding index transitions on the P2P link, which is an expected outcome.

## VII. CONCLUSION AND FUTURE WORK

A new, low-cost, automated, flexible testbed for interference susceptibility testing was demonstrated, characterized, and validated. The testbed design, validation methods, and accompanying public control software enable rapid implementation of similar testbeds for repeatable, reliable testing. ATIC allows for a wide range of noise and interference signals to be injected into a “closed-box” communication link by means of an SDR or other device with power levels controlled by a variable attenuator. Future work aims to leverage ATIC for further study of interference susceptibility and resultant behaviors for a diverse range of communication devices.

## ACKNOWLEDGMENT

This work was supported by the National Institute of Standards and Technology. MP was supported by the National Defense Science and Graduate Fellowship Program (NDSEG) through the University of Colorado Boulder.

## REFERENCES

- [1] Federal Communication Commission, “Advanced Wireless Services (AWS),” <https://www.fcc.gov/wireless/bureau-divisions/broadband-division/advanced-wireless-services-aws>, Last Updated: 2022-08-15.
- [2] —, “3.5 GHz Band Overview,” <https://www.fcc.gov/wireless/bureau-divisions/mobility-division/35-ghz-band/35-ghz-band-overview>, Last Updated: 2023-04-03.
- [3] R. J. Ulman, “ARL Broad Agency Announcements \*BAA: Wireless Communications Networks,” <https://cftste.experience.crmforce.mil>, Nov. 2022.
- [4] Department of Defense, “C3 Command, Control, and Communications Modernization Strategy,” Sept. 2020. [Online]. Available: <https://dodcio.defense.gov/Portals/0/Documents/DoD-C3-Strategy.pdf>
- [5] S. Futatsumori and N. Miyazaki, “Measurement of pulsed aircraft radio altimeter in-band and out-band interference threshold power due to sub-6 band 5G mobile communication systems,” in *2022 Int. Symposium on Electromagnetic Compatibility – EMC Europe*, 2022, pp. 608–611.
- [6] S. Bräuer, A. Zubow, and F. Dressler, “Towards software-centric listen-before-talk on software-defined radios,” in *2021 IEEE Wireless Communications and Networking Conference (WCNC)*, 2021, pp. 1–7.
- [7] S. Farrelly, “Rate vs. Range Test Methodology,” 2004. [Online]. Available: <https://mentor.ieee.org/802.11/dcn/04/11-04-1397-00-000t-rate-vs-range-test-methodology.ppt>
- [8] F. Mlinarsky, “Fundamentals of wireless test part 1: Range and roaming test,” 2012. [Online]. Available: <https://www.edn.com/fundamentals-of-wireless-test-part-1-range-and-roaming-test/>
- [9] 5G Americas, “C3 Command, Control, and Communications Modernization Strategy,” Feb. 2023. [Online]. Available: <https://www.5gamericas.org/wireless-receiver-performance/>
- [10] W. Young, D. McGillivray, A. Wunderlich, M. Krangle, J. Sklar, A. Sanders *et al.*, “AWS-3 LTE Impacts on Aeronautical Mobile Telemetry,” National Institute of Standards and Technology, Gaithersburg, MD, Tech. Rep. Technical Note 2140, Feb 2021.
- [11] W. F. Young, A. Feldman, S. M. Genco, A. Kord, D. G. Kuester, J. Ladbury *et al.*, “LTE Impacts on GPS,” National Institute of Standards and Technology, Gaithersburg, MD, Tech. Rep. Technical Note 1952, Feb 2017.
- [12] D. G. Kuester, A. Wunderlich, D. A. McGillivray, D. Gu, and A. K. Puls, “Blind Measurement of Receiver System Noise,” *IEEE Transactions on Microwave Theory and Techniques*, vol. 68, no. 6, pp. 2435–2453, 2020.
- [13] B. Vu, J. D. Mitchell, K. Stowell, M. Rabe, O. Huang, R. Lychev, and M. Kalke, “Mission resilience experimentation and evaluation testbed,” in *Proc. 2022 IEEE Military Communications Conference (MILCOM)*, 2022, pp. 173–179.
- [14] Ettus, “Ettus USRP X410 Specifications,” Ettus. [Online]. Available: <https://www.ni.com/docs/en-US/bundle/ettus-usrp-x410-specs/page/specs.html>
- [15] LigoWave, “LigoPTP 6-N/6-25 RapidFire,” LigoWave. [Online]. Available: <https://www.doubleradius.com/site/stores/ligowave/ligowave-ligoptp-6-n-rapidfire-datasheet.pdf>
- [16] Mini-Circuits, “Programmable attenuator RC4DAT-8G-95,” Mini-Circuits, Brooklyn, New York, United States. [Online]. Available: <https://www.minicircuits.com/pdfs/RC4DAT-8G-95.pdf>
- [17] E. D. Nelson and D. A. McGillivray, “In-Situ Captures of AWS-1 LTE for Aeronautical Mobile Telemetry System Evaluation,” National Telecommunications and Information Administration, Boulder, CO, Tech. Rep. 21-553, March 2021. [Online]. Available: <https://its.ntia.gov/publications/details.aspx?pub=3262>
- [18] A. Sanders, “In-Situ Captures of AWS-1 LTE,” <https://doi.org/10.18434/mds2-2413>.
- [19] D. C. Montgomery, *Design and Analysis of Experiments*, 9th ed. Hoboken, NJ: John Wiley & Sons, 2017.